ELSEVIER

Journal of Organometallic Chemistry 571 (1998) 97–102

Journal of Organometallic Chemistry

Synthesis, structure and properties of hexamethyltrisilane-bridged biscyclopentadienyl tetracarbonyl di-iron

Wenhua Xie, Baiquan Wang, Shansheng Xu, Xiuzhong Zhou *

Department of Chemistry, Nankai University, Tianjin 300071, People's Republic of China

Received 03 June 1998; received in revised form 25 July 1998

Abstract

The reaction of hexamethyltrisilane-bridged biscyclopentadiene $C_5H_5(SiMe_2)_3C_5H_5$ with $Fe(CO)_5$ in refluxing xylene gave corresponding di-iron complexes $(SiMe_2)_3[\eta^5\text{-}C_5H_4Fe(CO)]_2(\mu\text{-}CO)_2$ (**1**) together with the $(Me_2SiSiMe_2)[\eta^5\text{-}C_5H_4Fe(CO)]_2(\mu\text{-}CO)_2$ (**2**) and $[Me_2Si(\eta^5\text{-}C_5H_4)Fe(CO)_2]_2$ (**3**). The crystal structure of **1** was determined by X-ray diffraction. The formation of the latter two products was discussed. Studies on the UV spectra of **1** and **2** and with $Me_2Si[\eta^5\text{-}C_5H_4Fe(CO)]_2(\mu\text{-}CO)_2$(**4**) indicated that the connection of Si–Si bonds with coordinated cyclopentadienyls resulted in significant red shifts in λ_{max} for the UV spectra of **1** and **2**. The electrochemistry of **1**, **2** and **4** was also examined.

Keywords: Fe–Fe bond; Bridged-cyclopentadiene; Crystal structure

1. Introduction

Bridged biscyclopentadienyl binuclear complexes have been of particular interest. They allow a systematic approach to the study of the interactions between two metal reaction sites in close proximity [1–4]. For some years we have been investigating the syntheses, structures and reactions of silane and siloxane-bridged biscyclopentadienyl binuclear transition metal complexes [5,6]. Recently, we have reported the syntheses of tetramethyldisilane-bridged biscyclopentadienyl di-iron complexes, $(Me_2SiSiMe_2)[\eta^5\text{-}Cp'Fe(CO)]_2(\mu\text{-}CO)_2$ (Cp′ = C_5H_5, C_5H_4Me, t-BuC_5H_4, C_5Me_4, indenyl, tetrahydroindenyl) and the novel thermal rearrangement reaction between Si–Si and Fe–Fe bonds [7–12] (Scheme 1).

To examine whether this reaction also takes place in systems with longer sila-bridge, the hexamethyltrisilane-bridged biscyclopentadienyl di-iron complex $(SiMe_2)_3[\eta^5C_5H_4Fe(CO)]_2(\mu\text{-}CO)_2$(**1**) was synthesized and its properties were studied.

2. Results and discussion

2.1. Synthesis and reactions

Hexamethyltrisilane-bridged biscyclopentadienyl Fe–Fe bond complex **1** was synthesized by heating $C_5H_5(SiMe_2)_3C_5H_5$ with $Fe(CO)_5$ in refluxing xylene. Note that the expected rearrangement product **5** was isolated. While for the disilane-bridged analogues, syntheses of binuclear Fe–Fe complexes were always accompanied more or less by thermal rearrangement reactions between their Si–Si and Fe–Fe bonds which lead to related rearrangement products [7–11]. What was unexpected was the isolation of two previously reported complexes $(Me_2SiSiMe_2)[\eta^5\text{-}C_5H_4Fe(CO)]_2(\mu\text{-}CO)_2$ (**2**) and $[Me_2Si(\eta^5\text{-}C_5H_4)Fe(CO)_2]_2$ (**3**) [7] (Scheme 2).

In order to find out how **2** and **3** were formed, the ligand $C_5H_5(SiMe_2)_3C_5H_5$ was characterized firstly by GC/MS spectra, which indicated that the ligand did not contain $C_5H_5Me_2SiSiMe_2C_5H_5$ at all. Secondly, the pure complex **1** was subjected to further refluxing. The result is revealing. Except extensive decomposition and

* Corresponding author. Fax: +86 22 23502458.

0022-328X/98/$ - see front matter
PII S0022-328X(98)00890-0

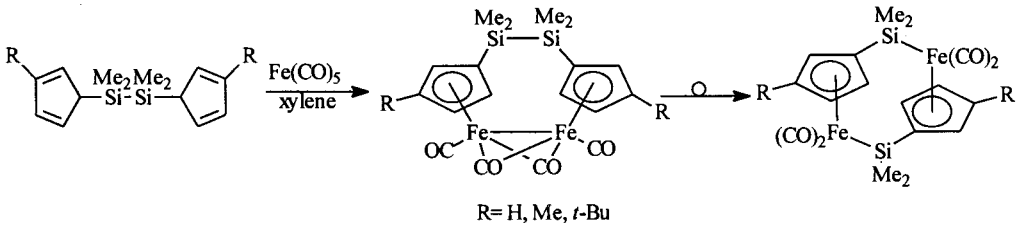

Scheme 1.

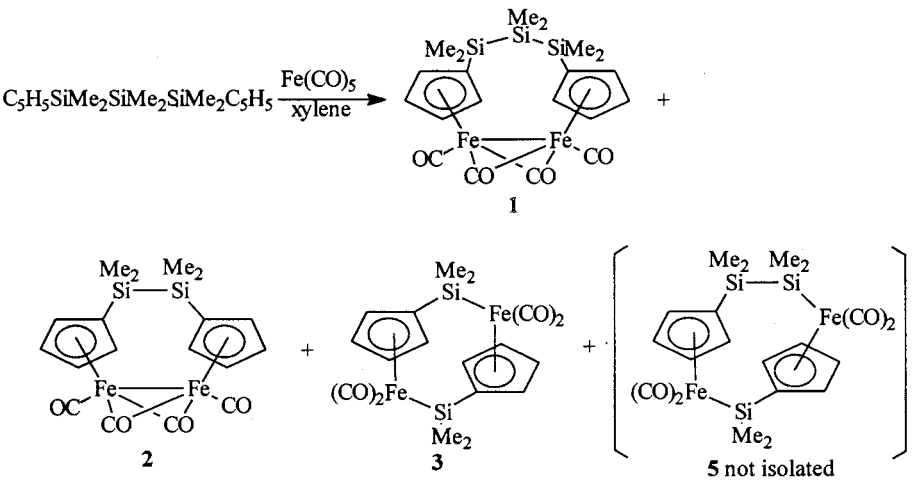

Scheme 2.

a very small amount of an unidentified oily substance in which IR spectrum no absorption of the carbonyl group existed, none of **2**, **3** or expected rearrangement product **5** was obtained. This firstly gave clear information that no reaction between Si–Si and Fe–Fe bonds took place for **1** (the same result can be expected for other trisilane-bridged analogues). Secondly, it indicated that **2** and **3** were not derived from **1**. It is reasonable to conclude that **3** came from the rearrangement of **2** which formed during the process of heating $C_5H_5(SiMe_2)_3C_5H_5$ with $Fe(CO)_5$, likely involving extrusion of a silylene from the polysilane backbone of the ligand.

Sakurai found that such a silylene extruction is general when carbonyliron compounds react with vinylsilanes [13,14] (Scheme 3).

Similarly, a possible mechanism of the formation of **2** could be suggested as following (Scheme 4):

Firstly, it is well known that a cyclopentadienylsilane is to exist as an equilibrium mixture consisting of the corresponding vinylsilane and allylsilane due to the extremely facile silyl and hydrogen shift around the cyclopentadienyl ring. The vinyltrisilane reacts with $Fe(CO)_5$ to form the π-complex which is transferred to the corresponding π-complex of the vinyldisilane with the elimination of the silylene unit under heat. After further reaction, including the hydrogen shift and elimination, **2** is formed as other Fe–Fe bond complexes.

2.2. Crystal structure of complex *1*

A full structure characterization for **1** was accomplished by X-ray crystallography. The structure of the molecule is illustrated in Figs. 1 and 2. The molecule has m symmetry. Si(2), C(11), Si(2a) and C(11a) are in a same plane and Si(1) swinging off the plane by 0.8359Å. The seven-membered ring C(11a)–Si(2a)–Si(1)–Si(2)–C(11)–Fe(1)–Fe(1a) takes a chair-like conformation. The dihedral angle between the two cyclopentadienyl ring planes is 97.53°. Si(2) deviates from the cyclopentadienyl plane by 0.331 7Å, more significantly than any of its disilane-bridged analogues. This is primarily due to the introduction of Si(1) which makes Si(2) and Si(2a) a little more apart while with a fixed Si–C bond distance. In addition, when crystallizing from CH_2Cl_2/pentane solution, the crystal of **1** contains two molecules of itself along with two molecules of CH_2Cl_2 in one unit cell.

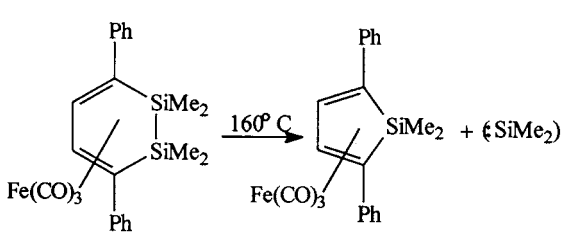

Scheme 3.

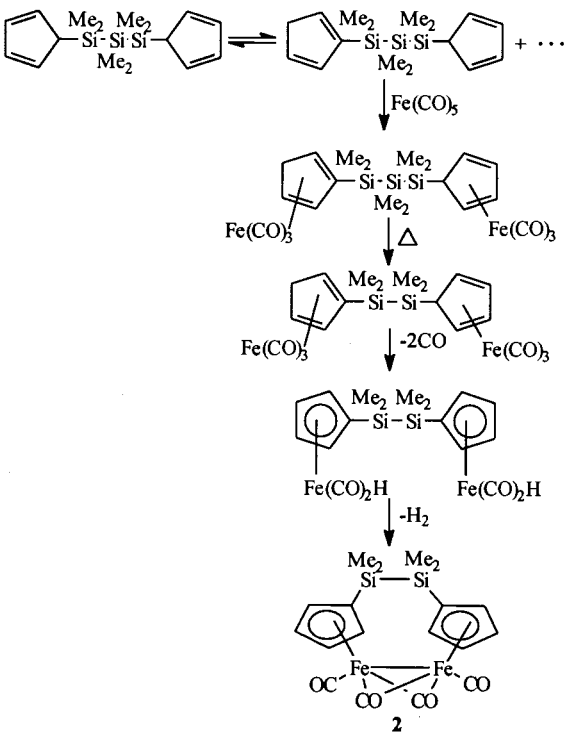

Scheme 4.

2.3. UV spectra

Studies on UV spectra of di-iron complexes **1**, **2** and $Me_2Si[\eta^5\text{-}C_5H_4Fe(CO)]_2(\mu\text{-}CO)_2$ (**4**) gave meaningful results. For all of them, there is one absorption assigned to the absorption of cyclopentadienyls at ~ 250 nm. As shown in Table 3, complexes **1** and **2**, compared with their unsubstituted analogue $[\eta^5\text{-}C_5H_5Fe(CO)]_2(\mu\text{-}CO)_2$, exhibit significant red shifts in λ_{max} ($\Delta\lambda_{max}$, 4 and 8 nm respectively), while for **4**, only a limited shift (1 nm). This is easily understood in terms of '$\sigma-\pi$' conjugation between Si–Si and π systems, which has been well recognized as an important factor responsible for conjugated properties in phenyl and vinyl substituted polysilanes [15,16]. Such $\sigma_{Si-Si}-\pi$ conjugation requires coplanarity between the pπ-axis and the interacting σ bond. In the molecule of **2**, the Si–Si bond, as shown by X-ray crystallography [7], is approximately perpendicular to the cyclopentadienyl rings. While in **1**, with Si(1) swinging off the plane defined by Si(2), C(11), Si(2) and C(11a), the Si–Si bond is in a slanted position, therefore, the $\sigma-\pi$ interaction is less effective. This is the reason why complex **2** displays a larger $\Delta\lambda_{max}$. These results add to our knowledge about $\sigma_{Si-Si}-\pi$ conjugation by indicating that such conjugation also happens for metal-coordinated π systems.

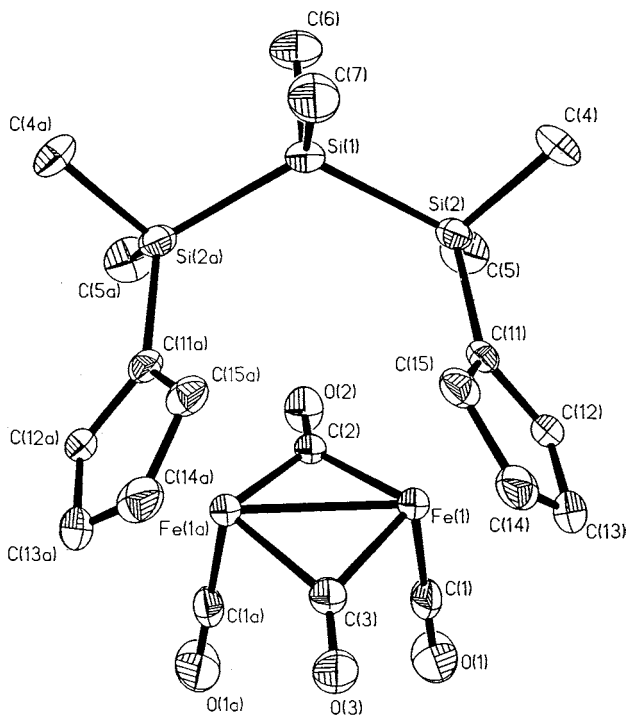

Fig. 1. The molecular structure of **1**.

2.4. Electrochemistry

The electrochemistry of complexes **1**, **2** and **4** has been investigated with cyclic voltammetry (CV) and potentiostatic coulometry. CV curves and CV data at different scan rates in (0.1 M $[NBu_4]PF_6$) dichloromethane solution at a platinum electrode are shown in Figs. 3 and 4 and Table 4. These results indicate partially reversible two-electron oxidation with reversibility $\mathbf{4} > \mathbf{2} > \mathbf{1}$. The sequence of reversibility connotes a similar sequence for stability of related dication: $[\mathbf{4}]^{2+} > [\mathbf{2}]^{2+} > [\mathbf{1}]^{2+}$. As the scan rate increases, the reversibility improves a lot. These electrochemical processes in CH_2Cl_2 for the three complexes are diffusion controlled with anodic current functions ($i_{pa}/\gamma^{1/2}$) independent approximately of the scan rate over the range of 0.5–5 V s^{-1}.

The electrochemical behavior of the complexes in CH_3CN shows great difference from that in CH_2Cl_2. The reversibility reduces remarkably. This is a little similar to what their siloxane-bridged analogues exhibit in THF [17]. As an example, Figs. 5 and 6 give, respectively, CV curves for oxidation and reduction of **2**. CV data are presented in Table 5. Thus, as these show, irreversible two-electron processes take place in CH_3CN for **1**, **2** and **4**.

3. Experimental

3.1. General

All operations were carried out in an argon atmosphere. THF and xylene were distilled from sodium

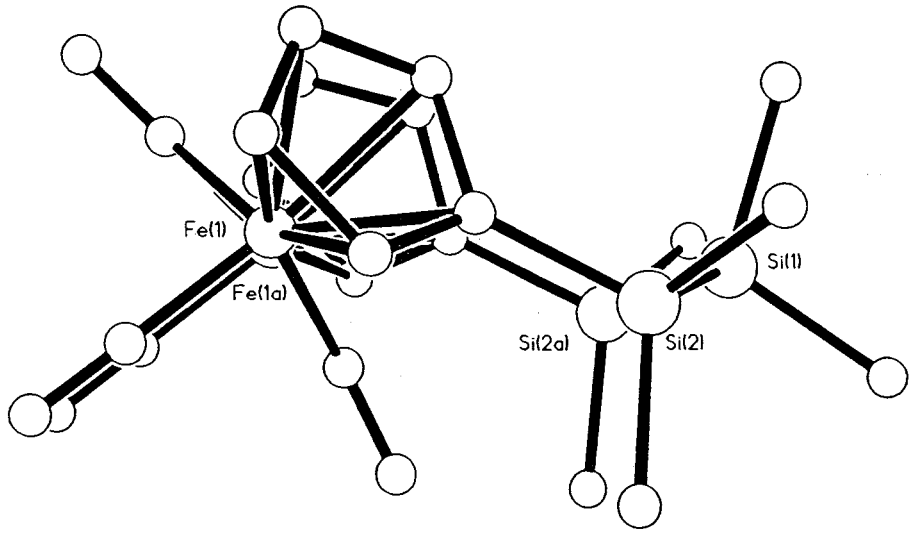

Fig. 2. A view of the molecule (**1**) along the Fe–Fe bond.

diphenylketyl under argon before use. CH_2Cl_2 was distilled from P_2O_5. CH_3CN was first refluxed with $KMnO_4$ and K_2CO_3, then distilled twice from P_2O_5. IR spectra were recorded on a Nicolet 5DX FT-IR spectrophotometer, while UV spectra on a Shimadzu UV-240, ^{1}H-NMR spectra on a BRUKER AC-P200 or JEOL FX-9OQ instrument.

Table 1
Summary of crystal data and data collection and refinement for $\mathbf{1}\cdot CH_2Cl_2$

Formula	$C_{21}H_{28}Cl_2Fe_2O_4Si_3$
M (g mol^{-1})	611.31
Crystal system	monoclinic
Space group	$P2_1/m$
a (Å)	6.813(4)
b (Å)	12.497(3)
c (Å)	16.129(2)
β (°)	92.60(2)
V (Å^3)	1372(1)
Z	2
$D_{calc.}$ (g cm^{-3})	1.48
$F(000)$	628
Crystal size (mm)	$0.2\times0.15\times0.35$
μ (Mo–K$_\alpha$) (mm^{-1})	1.407
Scan type	$\omega/2\theta$
θ range (°)	2.0–23.0
Reflections collected	2101
Independent reflections	1945
Observed reflections	1945
Observed reflections [$I\geq3\sigma$(I)]	1656
Number of refined parameters	175
Goodness of fit	4.1
Rint	0.015
Final R and Rw	0.056 and 0.056
Maximum Δ/σ	0.47
Maximum residual peak (e Å^{-3})	0.97

$Cl(SiMe_2)_3Cl$ was prepared from $Me_3SiSiMe_2SiMe_3$ [18] by literature method [19]. $Me_2Si[\eta^5$-$C_5H_4Fe(CO)]_2(\mu$-CO)2 (**4**) was also prepared by literature method [20].

3.2. Preparation of $C_5H_5(SiMe_2)_3C_5H_5$

A solution of $Cl(SiMe_2)_3Cl$ (15 g, 0.06 mol) in THF(20 ml) was added dropwise at room temperature to a THF solution of cyclopentadienyl sodium (0.12 mol). After 5 h of stirring, the reaction mixture was hydrolyzed with distilled water; routine work-up gave an orange oil. Chromatography on a SiO_2 column (30×3 cm) with petroleum ether(b.p. 30–60°C) afforded a pale yellow liquid, 13.7g. MS, m/z 304 (M^+, 39%). ^{1}H-NMR (90 MHz, $CDCl_3$): δ_H 0.08 (s, 12H), 0.16 (s, 6H), 3.10 (m, 2H), 6.50–6.78 (m, 8H).

3.3. Synthesis of **1**

A xylene solution of $C_5H_5(SiMe_2)_3C_5H_5$ (1.0 g, 3 mmol) and $Fe(CO)_5$ (0.8 ml, 6 mmol) was heated at reflux for 10 h. After removal of solvent under reduced pressure, the residue was extracted with CH_2Cl_2 and filtered through a short Al_2O_3 column (7×3 cm). Chromatography on a SiO_2 column (30×2.5 cm, ace-

Table 2
Selected bond distances (Å) and bond angels (°) of $\mathbf{1}\cdot CH_2Cl_2$

Fe(1)–Fe(1a)	2.5430(2)	Si(1)–Si(2)	2.3475(9)
Si(2)–C(11)	1.870(3)	Fe(1)–C(11)	2.165(2)
Fe(1)–C(2)	1.928	Fe(1)–C(3)	1.930
Si(1)–Si(2)–C(11)	114.84(9)	135.6 (1)	
Si(2)–2Si(1)–Si(2a)	122.2	Fe(1)–C(2)–Fe(1a)	82.5
Fe(1)–C(3)–Fe(1a)	82.4	PL(1)–PL(2)	97.53

PL, the plane of a five-membered ring.

Table 3
UV data for complexes **1**, **2** and **4** in CH_2Cl_2

Complex	λ_{max} (nm)	ε (l mol^{-1}·cm^{-1})
$[C_5H_5Fe(CO)_2]_2$	245	4.6×10^3
1	249	5.0×10^3
2	253	4.9×10^3
4	246	4.8×10^3

tone:petroleum ether, 1:5) gave first a yellow band, then two red ones. From the first red band 0.19 g of dark red crystals **1** was obtained in 12% yield. The other two bands afforded, respectively, 0.18 g of **3** (yield, 13%) and 0.11 g of **2** (yield, 8%).

1, Anal. found: C, 45.60; H, 5.05. $C_{20}H_{26}Fe_2O_4Si_3$ Cacl.: C, 45.64; H, 4.98%. ^{1}H-NMR ($CDCl_3$, 200 MHz): δ_H 0.25 (s, 6H), 0.37 (s, 12H), 4.36 (s, 4H) 5.30 (s, 4H). IR (KBr) (υ_{co}/cm^{-1}): 1753.5 vs, 1794.5 s, 1942.2 s, 1991.4 vs.

2, Anal. found: C, 46.10; H, 4.36. $C_{18}H_{20}Fe_2O_4Si_2$ Cacl.: C, 46.17; H, 4.31%. ^{1}H-NMR ($CDCl_3$, 90 MHz): δ_H 0.29 (s, 12H), 4.74 (s, 4H) 5.41 (s, 4H). IR (KBr) (υ_{co}/cm^{-1}): 1761.7 vs, 1797.0 s, 1942.1 s, 1991.4 vs.

3, Anal. found: C, 46.20; H, 4.40. $C_{18}H_{20}Fe_2O_4Si_2$ Cacl.: C, 46.17; H, 4.31%. ^{1}H-NMR ($CDCl_3$, 90 MHz): δ_H 0.48 (s, 12H), 5.02 (d, 8H). IR (KBr) (υ_{co}/cm^{-1}): 1975.0 vs, 1926.2 vs.

3.4. Thermal reaction of *1*

A xylene solution of **1** (0.25 g) was heated at reflux for 7 h. Extensive decomposition was observed from formation of insoluble deposit during the reaction. After removal of solvent in vacuum, chromatography of the residue on a SiO_2 column (20×2 cm) with CH_2Cl_2:petroleum ether (1:4) yielded only a very small amount of an unidentified yellow oil, which indicated no carbonyl absorption in its IR spectra.

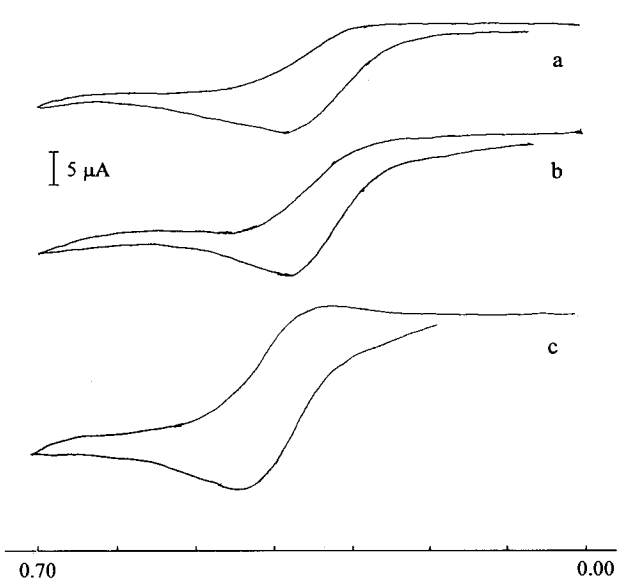

Fig. 3. Cyclic voltammograms in CH_2Cl_2 solution at Pt electrode (scan rate 0.1 V·s^{-1}) for (a) **1**, (b) **2**, and (c) **4**.

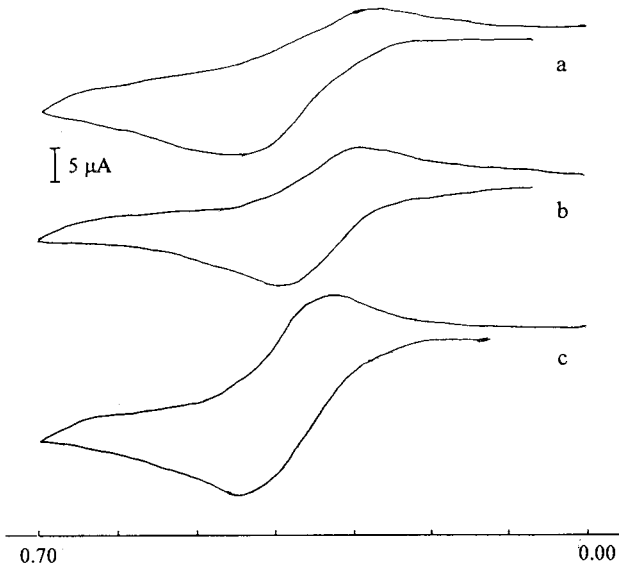

Fig. 4. Cyclic voltammograms at higher scan rates in CH_2Cl_2 solution at Pt electrode for (a) **1** at 5.12 V·s^{-1}, (b) **2** at 5.12 V·s^{-1}, and (c) **4** at 0.5 V·s^{-1}.

3.5. Crystallography

Crystals of **1** suitable for X-ray diffraction were obtained from CH_2Cl_2 + pentane solution at -20°C. Crystal data were collected at 299 K in the range $4.0° < 2\theta < 46.0°$ on an Enraf Nonius CAD4 diffractometer with Mo–K_α ($\lambda = 0.71073$ Å) radiation. Intensity data were corrected for the usual Lorentz and polarization effects; an empirical absorption correction was applied also. The structure was solved by direct method using the SDP-PLUS program. The full-matrix least-square method was employed for refinement. Crystal data and some details of data collection and refinement are given in Table 1. Selected bond lengths and bond angels are listed in Table 2.

3.6. Electrochemical measurements

A cell employing a three-electrode configuration is used in the electrochemical studies. A platinum wire with a radius of 0.1 mm or a glass-carbon electrode is used as the working electrode and a platinum wire serves as the counter electrode. All potentials are reported vs a $Ag\,|\,AgNO_3$ reference electrode. Cyclic voltammagrams were recorded at room temperature (in a solution containing 0.1 mol dm^{-3} $[NBu_4]PF_6$ as supporting electrolyte) on a BAS-100B recorder. In CH_3CN solutions, since it was unable to obtain satisfactory CV curves with a platinum electrode, a glass-carbon electrode was therefore employed.

Table 4
Cyclic voltammetric data[a] for complexes **1**, **2** and **4** in CH_2Cl_2

Complex	Scan rate (V s^{-1})	E_{p_a} (V)	E_{p_c} (V)	ΔE_p (V)	$i_{p/\gamma 1/2}$	i_a/i_c
1	0.5	0.26	0.12	0.14	1.20	2.73
	5	0.32	0.14	0.18	1.18	2.36
2	0.5	0.24	0.14	0.10	0.96	2.14
	5	0.26	0.14	0.12	1.01	1.68
4	0.5	0.30	0.19	0.11	0.64	1.55
	5	0.36	0.17	0.19	0.57	1.45

[a] At the platinum electrode. Potentials quoted vs $[Fe(\eta^5\text{-}C_5H_5)_2]^+/[Fe(\eta^5\text{-}C_5H_5)_2]$ couple.

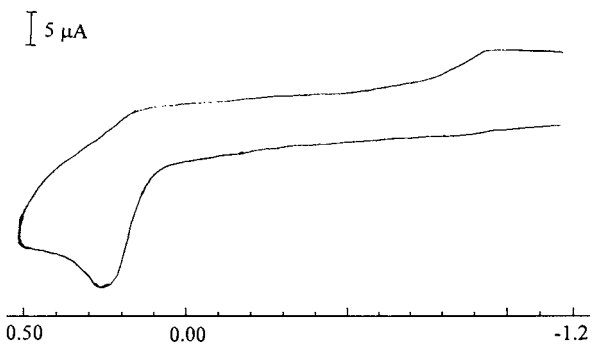

Fig. 5. Cyclic voltammograms for **2** in CH_3CN solution at glass-carbon electrode (oxidation, scan rate: 1 $V \cdot s^{-1}$).

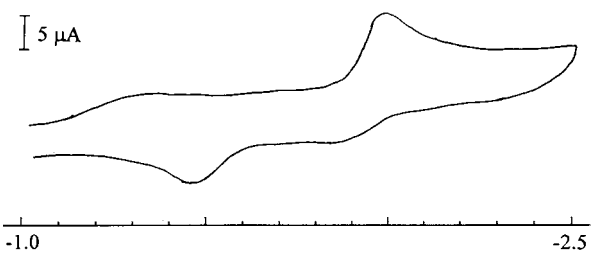

Fig. 6. Cyclic voltammograms for **2** in CH_3CN solution at glass-carbon electrode (reduction, scan rate: 1 $V \cdot s^{-1}$).

Table 5
Cyclic voltammetric data[a] for complexes **1**, **2** and **4** in CH_3CN at 1 V s^{-1}

Complex	Oxidation			Reduction		
	E_{p_a} (V)	E_{p_c} (V)	ΔE_p (V)	E_{p_c} (V)	$E_{p_{a1}}$ (V)	$E_{p_{a2}}$ (V)
1	0.21	−1.00	1.21	−2.02		−1.50
2	0.21	−1.02	1.23	−2.04	−1.87	−1.52
4	0.24	−0.99	1.23	−2.04	−1.91	−1.38

[a] At the glass-carbon electrode. Potentials quoted vs $[Fe(\eta^5\text{-}C_5H_5)_2]^+/[Fe(\eta^5\text{-}C_5H_5)_2]$ couple.

Acknowledgements

We greatly appreciate financial support from the National Natural Science Foundation of China and State Key Laboratory of Elemento-Organic Chemistry of Nankai University.

References

[1] R. Poilblanc, Inorg. Chem. Acta. 62 (1982) 75.
[2] W. Baumanu, W. Malish, J. Organomet. Chem. 303 (1986) 33.
[3] U. Siemeling, P. Jutzi, B. Neumann, H.G. Stammler, M.B. Hursthouse, Organometallics 11 (1992) 1328.
[4] C.G. Atwood, W.E. Geiger, A.L. Rheingold, J. Am. Chem. Soc. 115 (1993) 5310.
[5] X. Zhou, R. Jin, S. Xu, H. Wang, X. Yao, Acta Chim. Sin. 50 (1992) 930.
[6] W. Xie, X. Zhou, S. Xu, R. Wang, H. Wang, Acta Chim. Sin. 53 (1995) 1131.
[7] H. Sun, S. Xu, X. Zhou, J. Organomet. Chem. 404 (1993) 41.
[8] X. Zhou, C. Kong, S. Xu, Sci. Sin. B 23 (1993) 1133.
[9] X. Zhou, Y. Zhang, W. Xie, S. Xu, J. Sun, Organometallics 16 (1997) 3474.
[10] X. Zhou, X. Zhong, Y. Zhang, S. Xu, J. Organomet. Chem. 545–546 (1997) 435.
[11] B. Wang, S. Xu, X. Zhou, J. Organomet. Chem. 540 (1997) 101.
[12] B. Wang, Y. Zhang, S. Xu, X. Zhou, Organometallics 16 (1997) 4620.
[13] Y. Nakadaira, T. Kobayashi, H. Sakurai, J. Organomet. Chem. 165 (1979) 399.
[14] H. Sakurai, Y. Kamiyama, Y. Nakadaira, J. Organomet. Chem. 184 (1980) 13.
[15] H. Gilman, W.H. Atwell, J. Organomet. Chem. 4 (1965) 176.
[16] H. Sakurai, J. Organomet. Chem. 200 (1980) 261.
[17] M. Moran, I. Cuadrado, J.R. Masaguer, J. Chem. Soc. Dalton Trans. (1988) 833.
[18] H. Gilman, R.L. Harrell, J. Organomet. Chem. 5 (1966) 201.
[19] H. Sakurai, K. Tominaga, T. Watanabe, M. Kumada, Tetrahedron Lett. 45 (1966) 5493.
[20] J. Weaver, P. Woodward, J. Chem. Soc., Dalton Trans. (1973) 1439.